

ANTI-SOUND AND ACOUSTICAL CLOAKS

Veturia CHIROIU¹, Ligia MUNTEANU², Dan DUMITRIU³,
Cristian RUGINA⁴, Cornel BRISAN⁵

^{1,2,3}*Institute of Solid Mechanics, Romanian Academy, Bucharest, Romania*

¹veturiachiroiulie@gmail.com

²ligia_munteanu@hotmail.com

³dumitri04@yahoo.com

⁴*Technical University of Cluj-Napoca,*

Dept. of Mechatronics and System Dynamics, Romania

⁴rugina.cristian@gmail.com

⁵cornel.brisan@mmfm.utcluj.ro

Abstract

The principles by which the acoustics can be mimicked in order to reduce or cancel the vibrational field are based on anti-sound concept which can be materialized by acoustic cloaks. Geometric transformations open an elegant way towards the unconstrained control of sound through acoustic metamaterials. Acoustic cloaks can be achieved through geometric transformations which bring exotic metamaterial properties into the acoustic equations. Our paper brings new ideas concerning the technological keys for manufacturing of novel metamaterials based on the spatial compression of Cantor structures, and the architecture of 3D acoustic cloaks in a given frequency band, with application to architectural acoustics.

Keywords: anti-sound, acoustic cloak, metamaterial, Cantor structures

1. Introduction

The paper discusses the technological keys for manufacturing of novel metamaterials based on the spatial compression of Cantor structures, and the architecture of 3D acoustic cloaks in a given frequency band, with application to architectural acoustics. The theory is simple and consists in transformation of an original domain with a given shape filled with a known material (in our case an alternative layer of piezoelectric ceramics and epoxy resin following a triadic Cantor sequence) into a final domain, by applying a specific geometric transformation. The final domain will have a desired shape and will be filled with a new desired material, strongly inhomogeneous and anisotropic. This new metamaterial must be engineered at the subwavelength scale in order to imitate the exotic properties provided by the wave equations. The exotic properties of the metamaterial are ideal and complex, being real challenges to experimentalists, but not impossible to be fabricated. The current limitation on acoustic metamaterials is fabrication. Comprehensive technical reviews are available in [1-6]. Our task is to propose a virtual robust simulation technology of manufacturing which could be applied

in practice to low cost. This technology consists in developing of 3D Cantor helices of this material. These 3D structure are arranged on superposed 2D different size and shape lattices. The nanostructures can be fabricated via the approach based on direct laser writing into a photoresist positive tone followed by electrochemical deposition of Cantor helices [7].

2. Anti-sound and geometric transformations

The sounds are mechanical vibration of the air and the ear is sensing the pressure and its gradient fluctuations. Two pressure fields arranged to overlap precisely with exactly opposite characteristics in waves can destroy by interfering the sound, producing a constant pressure which is the condition of silence. This silence can be viewed as the superposition of sound and anti-sound [6]. The same effect can be obtained by surrounding the noise source by a cloak so that sound incident from any direction passes through and around the cloak, making the cloak and the object acoustically invisible. The materials required for constructing the cloak are exotic and they are not found in nature. Simply mathematics is necessary to understand the concept of geometric transformation which defines the type of

metamaterial required. The 3D acoustic equation for the pressure waves propagating in a bounded air region $\Omega \subset \mathbb{R}^3$ is

$$\nabla \cdot (\underline{\underline{\rho}}^{-1} \nabla \pi) + \frac{\omega^2}{\kappa} \pi = 0, \quad (1)$$

where p is the pressure, $\underline{\underline{\rho}}$ is the rank-2 tensor of the fluid density, κ is the compression modulus of the fluid, and ω is the wave frequency. Let us consider the geometric transformation from the coordinate system (x', y', z') of the compressed space to the original coordinate system (x, y, z) , given by $x(x', y', z')$, $y(x', y', z')$ and $z(x', y', z')$. The change of coordinates is characterized by the transformation of the differentials through the Jacobian $J_{xx'}$ of this transformation, i.e.

$$\begin{pmatrix} dx \\ dy \\ dz \end{pmatrix} = J_{xx'} \begin{pmatrix} dx' \\ dy' \\ dz' \end{pmatrix}, \quad J_{xx'} = \frac{\partial(x, y, z)}{\partial(x', y', z')}. \quad (2)$$

From the geometrical point of view, the change of coordinates implies that, in the transformed region, one can work with an associated metric tensor

$$T = \frac{J_{xx'}^T J_{xx'}}{\det(J_{xx'})}. \quad (3)$$

In terms of the acoustic parameters, one can replace the material from the original domain (homogeneous and isotropic) by an equivalent compressed one that is inhomogeneous (its characteristics depend on the spherical (r', θ', ϕ') coordinates) and anisotropic (described by a tensor), and whose properties, in terms of $J_{xx'}$, are given by

$$\begin{aligned} \underline{\underline{\rho}}' &= J_{xx'}^{-T} \cdot \underline{\underline{\rho}} \cdot J_{xx'}^{-1} \cdot \det(J_{xx'}), \\ \kappa' &= \kappa \det(J_{xx'}), \end{aligned} \quad (4)$$

or, equivalently, in terms of $J_{xx'}$

$$\underline{\underline{\rho}}' = \frac{J_{xx'}^T \cdot \underline{\underline{\rho}} \cdot J_{xx'}}{\det(J_{xx'})}, \quad \kappa' = \frac{\kappa}{\det(J_{xx'})}. \quad (5)$$

Here, $\underline{\underline{\rho}}'$ is a second order tensor. When the Jacobian matrix is diagonal, (4) and (5) can be more easily written. Multiplying (1) by a test function φ and integrating by parts, one obtains [6]

$$\begin{aligned} -\int_{\Omega} \left(\nabla_{(x,y,z)} \varphi \cdot \underline{\underline{\rho}}^{-1} \nabla_{(x,y,z)} p \right) dV + \\ + \int_{\Omega} \left(\omega^2 \kappa^{-1} p \varphi \right) dV = 0, \end{aligned} \quad (6)$$

In (6) the surface integral, corresponding to a Neumann integral over the boundary $\partial\Omega$, is zero. By applying the coordinate transformation

$(x, y, z) \rightarrow (x', y', z')$ to (6) and using (2), one obtains

$$\begin{aligned} -\int_{\Omega} \left(J_{xx'}^T \nabla_{(x',y',z')} \varphi \cdot \underline{\underline{\rho}}^{-1} J_{xx'}^T \nabla_{(x,y,z)} p \right) \det(J_{xx'}) dV' + \\ + \int_{\Omega} \left(\det(J_{xx'}) \omega^2 \kappa^{-1} p \varphi \right) dV' = 0, \end{aligned} \quad (7)$$

in terms of $J_{xx'}$, and

$$\begin{aligned} -\int_{\Omega} \left(\left(\nabla_{(x',y',z')} \varphi \right)^T \frac{J_{xx'} \underline{\underline{\rho}}^{-1} J_{xx'}^T}{\det(J_{xx'})} \nabla_{(x',y',z')} p \right) dV' + \\ + \int_{\Omega} \left(\frac{\kappa^{-1}}{\det(J_{xx'})} \omega^2 p \varphi \right) dV' = 0, \end{aligned} \quad (8)$$

in terms of $J_{xx'}$.

3. Spherical acoustic cloak

Our intention is to replace a material made from concentric homogeneous and isotropic layers situated in the original spherical domain by an equivalent compressed inhomogeneous anisotropic material described by the transformation matrix (3). Let us suppose that the original domain Ω is a sphere of radius R_2 . The sphere consists of an alternation of concentric layers made from piezoelectric ceramics and epoxy resin, following a triadic Cantor sequence up to the fourth generation (31 elements). The original domain is a sphere of radius R_2 , consisting of alternation of concentric layers made from piezoelectric ceramics and epoxy resin, following a triadic Cantor sequence (Fig.1b). After the transformation, the cloak contains a region $r < R_1$ filled with air and containing the noisy source, while the shell $R_1 < r < R_2$ is filled by the nonlinear transformed material.

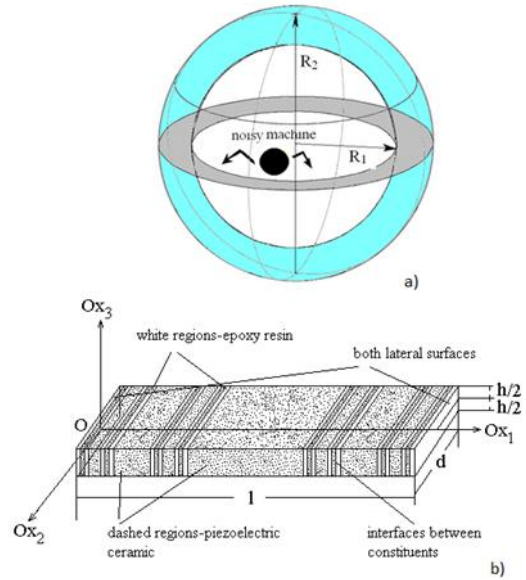


Fig. 1: (a) Sketch of spherical cloak surrounding a

noisy machine; (b) Cantor-like structure [1].

Next, the governing equations of this composite are written in the spirit of [9-12]. The quasistatic motion equations and constitutive laws read as

$$\rho \ddot{u}_i = t_{ij,j}, \quad (9)$$

$$D_{i,i} = 0, \quad E_i + \varphi_{e,i} = 0. \quad (10)$$

Here, indices p and e denote the piezoelectric (PZ) and non-piezoelectric (ER) materials, respectively, ρ is the density, u_i , $i=1,2,3$, are the components of the displacement vector, t_{ij} , $i=j=1,2,3$, are the components of the stress tensor, D_i , $i=1,2,3$, are the components of the electric induction vector, E_i , $i=1,2,3$, are the components of the electric field and φ_e is the electric potential, ε_{ij} , $i=j=1,2,3$, are the components of the strain tensor, λ , μ are the Lamé constants, $\bar{\varepsilon}^p$ is the dielectric constant and e_i^p ($e_3^p = e_2^p = e_1^p$) are the piezoelectricity coefficients. The coordinate x_1 is directed along the radial direction, x_3 is directed along the circumferential direction, while x_2 is located within the layer.

$$t_{ij} = \lambda^p \varepsilon_{kk} \delta_{ij} + 2\mu^p \varepsilon_{ij} - e_k^p E_k \delta_{ij}, \quad (11)$$

$$t_{ij} = \lambda^e \varepsilon_{kk} \delta_{ij} + 2\mu^e \varepsilon_{ij}, \quad (12)$$

$$D_i = \bar{\varepsilon}^p E_i - e_i^p \varepsilon_{kk}, \quad (13)$$

$$\varepsilon_{ij} = \frac{1}{2}(u_{i,j} + u_{j,i}), \quad (14)$$

The scalar elastic potential φ , and the components ψ_1 , ψ_2 , ψ_3 of the vectorial elastic potential, defined as

$$u_1 = \varphi_{,1} - \psi_{2,3}, u_2 = \psi_{1,3} - \psi_{3,1}, u_3 = \varphi_{,3} + \psi_{2,1}, \quad (15)$$

and the electric potential φ_e , are expressed using the theta-function [12]

$$\varphi(x_1, x_2, x_3, t) = \varphi_0(t) \Delta(\log \Theta(x_1, x_2, x_3)),$$

$$\psi_i(x_1, x_2, x_3) = \psi_{i0}(t) \Delta(\log \Theta(x_1, x_2, x_3)),$$

$$\varphi_e(x_1, x_2, x_3) = \varphi_{e0}(t) \Delta(\log \Theta(x_1, x_2, x_3)). \quad (16)$$

On adopting the hypothesis of the theory of Von-Karman, the theta function Θ is the solution of the von Karman equation

$$\nabla \cdot \zeta_{p,e}^{-1} \nabla (\Delta \nabla \cdot \zeta_{p,e}^{-1} \nabla \Theta) - \Lambda^{-1} \gamma_0^4 \Theta = 0, \quad (17)$$

where $\zeta = E^{-1/2}$, E is the effective Young modulus of the composite, $\gamma_0^4 = \omega^2 \rho h / D_0$, D_0 is the flexural rigidity of the plate, ρ its effective density, h its thickness, $\Lambda = \rho^{-1}$ and ω the frequency. Eq. (3.9) can be factorized as a Helmholtz operator and an anti-Helmholtz operator (i.e. with an opposite sign for the spectral parameter)

$$(\nabla^2 + \gamma_0^2)(\nabla^2 - \gamma_0^2)\Theta = 0, \quad (18)$$

where for simplicity we have taken $\zeta = \Lambda = 1$. We write the Helmholtz equation in the coordinate system (x_1, x_2, x_3) as

$$\nabla \cdot (\zeta^{-1} \nabla \Theta) + \omega^2 \Lambda^{-1} \Theta = 0. \quad (19)$$

Let us apply the concave-down transformation (2) and (3) to (17), which compresses the original domain Ω occupied by a sphere of radius R_2 into a shell region $R_1 < r' < R_2$ in the compressed space Ω' , characterized by

$$\begin{aligned} \underline{\zeta}_{p,e}^{r-1}(r') &= J_{rr'}^T \zeta_{p,e}^{-1}(r) J_{rr'} / \det(J_{rr'}), \\ (20) \quad \underline{\Lambda}^{r-1}(r') &= J_{rr'}^T \Lambda^{-1}(r) J_{rr'} / \det(J_{rr'}), \quad J_{rr'} = \partial r / \partial r', \end{aligned} \quad (21)$$

In the new coordinates, the transformed equation (17) now reads as

$$\nabla \cdot \underline{\zeta}_{p,e}^{-1} \nabla (\Delta_{33} \nabla \cdot \underline{\zeta}_{p,e}^{-1} \nabla \Theta') - \Lambda_{33}^{-1} \gamma_0^4 \Theta' = 0, \quad (22)$$

where $\underline{\zeta}_{p,e}^{-1}$ is the upper diagonal part of the inverse of $\underline{\zeta}$ and Λ_{33}^{-1} is the third diagonal entry of $\underline{\Lambda}^{-1}$ [13].

The cloak has the inner radius $R_1 = 0.5\text{m}$ and outer radius $R_2 = 1\text{m}$. After simulation [1], the absence of the scattering of waves generated by external source outside the cloak is observed in Fig. 2. The waves are smoothly bent around the central region inside the cloak. The results reported show that the wave field inside the cloak, i.e. the inner region of radius R_1 which surrounds the noisy machine, is completely isolated from the region situated outside the cloak.

The waves generated by a noisy source are smoothly confined inside the inner region of the cloak. The inner region is acoustically isolated and the sound is not detectable by an exterior observer because the amplitudes on the boundary vanish.

The domain is an acoustic invisible domain for exterior observers. The waves generated by the exterior source outside the cloak do not interact with the interior field of waves.

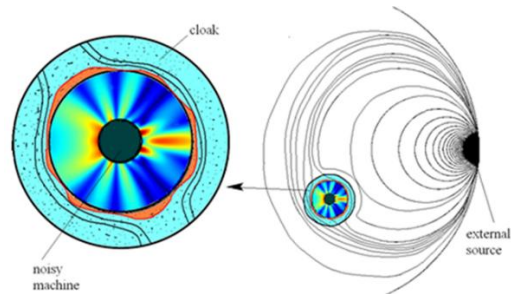


Fig. 2: Waves fields inside and outside the cloak [1].

A possible interaction or coupling the internal and external wave fields is cancelled out by the presence of the shell region $R_1 < r < R_2$ filled with metamaterial. Hence we can conclude that the

concave-down spherical cloaks lead to a smaller disturbance in the acoustic fields in both the inner and the outer spaces $r < R_2$ and $r > R_2$, respectively.

In this way, 3D omnidirectional acoustic cloaks can be constructed and the results are spectacular: outside of the cloak we do not hear anything like the noise source did not exist. Acoustic wavelengths have orders of magnitude larger than optical wavelengths, meters vs. microns, which makes the acoustic problem easier to be investigated.

4. Vibrational regimes

We start with the resonant vibration modes excited by applying an external electric field $\vec{E}^1 = \vec{E}_3 = \vec{E}^0 \exp(i\omega_0 t)$ on both sides of the plate with $\omega = \omega_n$. If \vec{E}^0 is increased above a threshold value $\vec{E}_{th}^0 = 5.77V$ the $\omega/2$ subharmonic generation is observed. In [14] the authors obtain in the Cantor-like sample typical values of the lowest threshold voltages of 3-5V. The amplitude of waves is calculated at the surface of the plate as a function of \vec{E}^0 . Figs.3 and 4 show the displacements of the normal modes $\omega/2\pi = 0.332\text{MHz}$, 0.550MHz and respectively of the subharmonic modes $\omega/4\pi = 166\text{MHz}$, 0.275MHz . Two kinds of vibration regimes are found: a localised-mode (fracton) regime represented in Fig.5 for $\omega/2\pi = 1.223\text{MHz}$, 1.964MHz and 2.340MHz , and an extended-vibration (phonon) regime represented in Fig.6 for $\omega/2\pi = 3.109\text{MHz}$ and 3.422MHz . A sketch of the plate geometry is given on the abscissa (dashed, piezoelectric ceramic and white, epoxy resin).

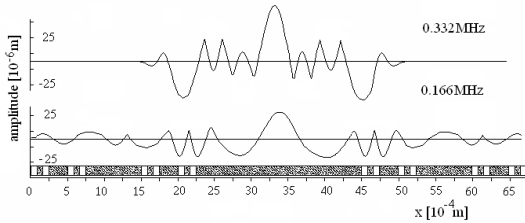


Fig.3: Amplitudes of the surface displacement of the normal mode $\omega/2\pi = 0.332\text{MHz}$ and the subharmonic mode $\omega/4\pi = 0.166\text{MHz}$

The fracton vibrations are mostly localised on a few elements, while the phonon vibrations essentially extend to the whole plate. In the case of a periodical plate the dispersion prevents good frequency matching between the fundamental and appropriate subharmonic modes. For the homogeneous plate the mismatch $\omega_n - \omega/2$ is due to the symmetry of fundamental modes with respect to x .

Only symmetric odd n can induce a subharmonic, but never $\omega/2$ coincides with a plate vibration mode.

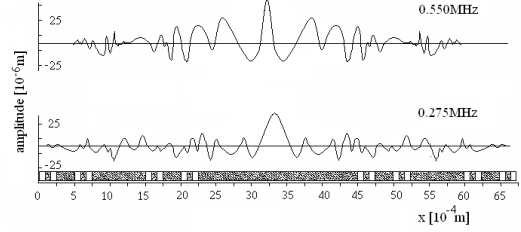


Fig.4: Amplitudes of the surface displacement of the normal mode $\omega/2\pi = 0.550\text{MHz}$ and the subharmonic mode $\omega/4\pi = 0.275\text{MHz}$.

For a Cantor-like plate, we have obtained qualitatively the same result as in [15]: given a normal mode ω_n , for excitation at $\omega = \omega_n$, the value of the expected threshold E_{th} i. e. the ability of generating the $\omega/2$ subharmonic, is determined by the existence of a normal mode with: (i) small frequency mismatch $\omega_n - \omega/2$, and, (ii) large spatial overlap between the fundamental and subharmonic displacement field.

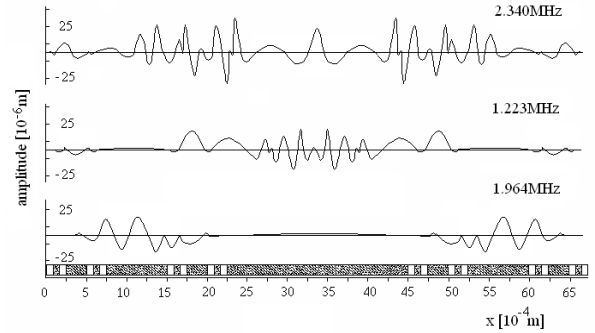


Fig.5: The normal amplitudes for three localised vibration modes ($\omega/2\pi = 1.223\text{MHz}$, 1.964MHz and 2.340MHz).

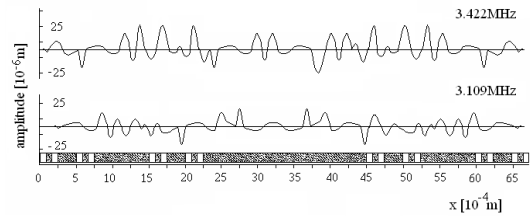


Fig.6: The normal amplitudes for two extended vibration modes ($\omega/2\pi = 3.109\text{MHz}$ and 3.422MHz).

5. Virtual simulation of the metamaterial manufacturing

The problem of manufacturing of novel metamaterial obtained by spatial compression from a Cantor structure, is solved in two stages. The first stage consists in virtual manufacture and architecture of a novel class of metamaterials based on Cantor structure.

Recipe for novel metamaterials are the geometric transformations (1)-(3) and generation of 3D Cantor

helices as a superposition of 2D lattices (Fig.7).

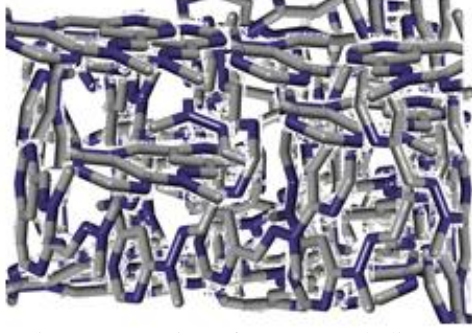


Fig.7: Generation of 3D Cantor helices.

The central hypothesis of generation of 3D Cantor helices is that the superposition at the point P of 2D different lattices is not a function of the smoothed (homogenized) mapping at the same point, but a function of the shape and size of the lattice over a certain characteristic volume centred at that point, the size of which is the characteristic length l

$$\sigma = F(\bar{\varepsilon}(z)),$$

$$\bar{\varepsilon}(z) = \frac{1}{l} [u(z + \frac{l}{2}) - u(z - \frac{l}{2})] = \frac{1}{l} \int_{-l/2}^{l/2} \varepsilon(z + s) ds, \quad (4)$$

here $z \equiv X_3$ represents the modulation direction.

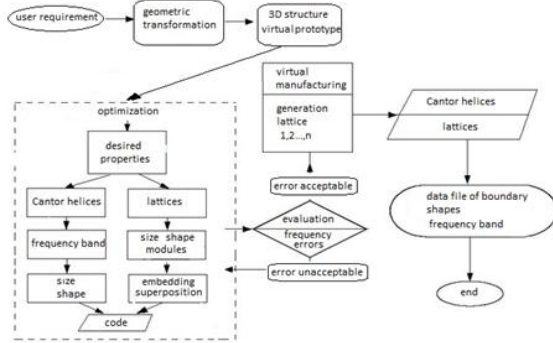


Fig. 8: The workflow of the virtual manufacturing of the metamaterial

So, we define the mean function of superposition as a certain averaging integral over the characteristic volume V

$$\bar{\varepsilon} = \frac{1}{V} \int_V \varepsilon(x') dV, \quad (5)$$

with V a sphere of radius $l/2$ centred in the point P. We suppose the modulation law is $A \sin(2\pi z/\lambda)$. The condition of coherency of the superposition establishes that, at this location, lattices A and B have the same in-plane lattice spacing. Away from the layers where the function $\bar{\varepsilon}$ attains a maximum, the structure relaxes towards its unstrained condition. The lattices are bounded by interfaces; therefore, the location of the minimum of the function $\bar{\varepsilon}$ is at the lattice centre. The functional variation with respect to z is

$$\bar{\varepsilon}(z) = \varepsilon_0 (1 + \cos(\frac{4\pi z}{\lambda})), \quad \varepsilon(z + \lambda) = \varepsilon(z), \quad (6)$$

where ε_{i0} is the maximum value of $\bar{\varepsilon}$.

The workflow of the virtual manufacturing of the metamaterial is presented in Fig. 8. Nanostructures can be fabricated via an approach based on direct laser writing into a positive-tone photoresist and electrochemical deposition of Cantor helices.

6. Reconfigurability and variable geometry

The structure and shape of the cloak are elaborated by using reconfigurability and variable geometry concepts [16, 17]. The concept is different from anechoic coatings because in our case we get a wide frequency band for which the cloak creates a 3D spatial region, invisible to sound. Thereconfigurability and variable geometry concepts play an important role in modifying properties of acoustic cloaks. Two different cloaks surrounding a noise object are presented in Fig. 9. The cloak can be built as a complex chain of modules with different shapes, and the nanoscale physical processes are able to manipulate its behavior in air, water and earth. Also, it offers a good alternative for the development of reconfigurable cloaks with different geometric shapes and multiple functionalities.

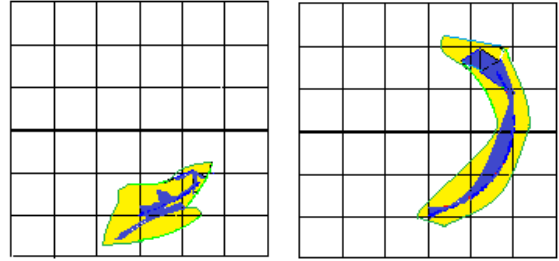


Fig. 9: Two different cloaks surrounding a noise object.

The acoustic properties of cloaks can be easily changed by precisely manipulating of properties furnished by the wave equations. As a result, a number of innovative cloaks can be developed.

7. Passive and active cloaks

Next, the passive and active cloaks for sound cancellation are considered on the base of nonlocal impedance coating extended reactions [18-21].

Passive cloaking requires complex metamaterials in order to manipulate the wave motion around a region, while active cloaking uses sources of sound to cancel the waves. Active cloaking is closely related to active noise control and anti-sound which reduces the radiating field or creates quiet regions in enclosed domains such as aircraft cabins.

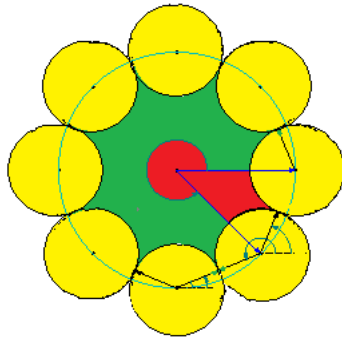


Fig. 10: Typical configuration for eight active sources [19].

Active cloaking requires knowledge of the incident field in order to activate wave sources (sources must be non-radiating) that cancel the total field in a given region. In addition, the cloaked region is not completely surrounded by a single cloak and a small number of active sources are required. Typical configuration for eight active sources is presented in Fig. 10[21]. The cloaking effect is independent on the location of the scatterers.

8. Conclusions

The paper is discussing the technological key for manufacturing of novel metamaterials based on the spatial compression of Cantor structures, and architecture of 3D acoustic cloaks in a given frequency band for application to architectural acoustics. The theory consists in transformation of an original domain with a given shape filled with a known material (in our case an alternative layer of piezoelectric ceramics and epoxy resin following a triadic Cantor sequence) into a final domain, by applying a geometric transformation. Final domain will have desired shape and will be filled with desired material, inhomogeneous and anisotropic. Exotic properties provided by the wave equations are ideal and complex, being real challenges to experimentalists given that the current limitation on metamaterials is fabrication. The task is to develop a virtual robust simulation technology which could be applied to low cost. This technology consists in developing of 3D Cantor helices by superposing of 2D lattices of different size and shape.

Acknowledgement. The authors gratefully acknowledge the financial support of the National Authority for Scientific Research ANCS/UEFISCDI through the project PN-II-ID-PCE-2012-4-0023 Contract nr.3/2013 and the project PN-II-PT-PCCA-2011-3.1-0190 Contract nr.149/2012. The authors acknowledge the similar and equal contributions to this article.

References

[1] Munteanu L. and Chiroiu V. (2011), *On the three-dimensional spherical acoustic*

cloaking, *New Journal of Physics*, 13 (8), 083031.

- [2] Pendry, J., Luo, Y. and Zhao, R. (2015), *Transforming the optical landscape*, *Science* 348, 521–524.
- [3] Luo, Y., Zhao, R. and Pendry, J.B. (2014), *Van der Waals interactions at the nanoscale: The effects of nonlocality*, *Proceedings of the National Academy of Sciences of the United States of America*, Vol. 111, 18422-18427.
- [4] Zigoreanu, L., Popa, B.I. and Cummer, A. (2014), *Three-dimensional broadband omnidirectional acoustic ground cloak*, *Nature Materials*, 13, 352-355.
- [5] Silva, A., Monticone, F., Castaldi, G., Galdi, V., Alù, A. and Engheta, N. (2014), *Performing Mathematical Operations with Metamaterials*, *Science* 343, 6167, 160-163.
- [6] Ffwcs, J.E.W. (1984), *Review Lecture: Antisound*, *Proc. R. Soc. Lond. A* 395, 63-88.
- [7] Dupont, G., Farhat, M., Diatta, A., Guenneau, S. and Enoch, S. (2011), *Numerical analysis of three-dimensional acoustic cloaks and carpets*, *Wave Motion* 48 (6), 483–496.
- [8] Gansel, K., Thiel, M., Rill, M.S., Decker, M., Bade, K., Saile, V., von Freymann, G., Linden, St. and Wegener, M. (2009), *Gold Helix photonic metamaterial as broadband circular polarizer*, *Science*, 325(5947), 1513-1515.
- [9] Truesdell, C. (ed.) (1974) *Handbuch der Physics*, Bd. VI a /4, Berlin, Springer.
- [10] Rogacheva, N.N. (1994), *The Theory of Piezoelectric Shells and Plates*, Boca Raton: CRC Press.
- [11] Landau L.D. and Lifshitz E. M. (1982), *Electrodynamics of Continuous Media*, Moscow, Nauka in Russian, translated into English Oxford, Pergamon Press 1984.
- [12] Chiroiu, C., Delsanto, P.P., Scalerandi, M., Chiroiu, V. and Sireteanu, T. (2001), *Subharmonic generation in piezoelectrics with Cantor-like structure*, *Journal of Physics D: Applied Physics*, Institute of Physics Publishing, 34(3), 1579–1586.
- [13] Guenneau, S., McPhedran, R.C., Enoch, S., Movchan, A.B., Farhat, M., Nicorovici, N.A. (2011), *The colours of cloaks*, *Journal of Optics*, 13, 2, 024014.
- [14] Alippi, A., Shkerdin, G., Bertucci, A., Craciun, F., Molinari, E. and Petri, A. (1992), *Threshold lowering for subharmonic generation in Cantor composite structures*, *Physica A* 191(1-4), 540–544.
- [15] Craciun, F., Bettucci, A., Molinari, E., Petri, A. and Alippi, A. (1992), *Direct experimental observation of fracton mode patterns in one-dimensional Cantor composites*, *Phys. Rev. Lett.* 68 (10).
- [16] Brisan, C., Vasii, R.V. and Munteanu, L. (2013), *A modular road auto-generating*

- algorithm for developing the road models for driving simulators*, Transportation Research Part C: Emerging Technologies, vol. 26, no. C, p. 269–284.
- [17] Csiszar, A., Boanta, C., Hoher, S., Brisan, C. and Verl, A. (2014), *Optimal Design Concept of a Reconfigurable Haptic Device*, Cham: Springer International Publishing, p. 267–272.
- [18] Bobrovnitskii, Y. (2010), *Impedance acoustic cloaking*, New Journal of Physics 12, 043049+.
- [19] Bobrovnitskii, Y. (2004), *A new solution to the problem of an acoustically transparent body*, Acoustical Physics, 50(6), 647–650.
- [20] Chen, H., Wu, B.I., Zhang, B. and Kong, J.A. (2007) *Electromagnetic wave interaction with a metamaterial cloak*, Physical Review Letters, 99, 063903.
- [21] Futhazar, G., Parnell W.J and Norris A.N. (2015), *Active cloaking of flexural waves in thin plates*, J. of Sound and Vibration, 356, 1-19.